

A C216-Nanographene Molecule with Defined Cavity as Extended Coronoid

Uliana Beser,[†] Marcel Kastler,^{†,§} Ali Maghsoumi,[‡] Manfred Wagner,[†] Chiara Castiglioni,[‡] Matteo Tommasini,[‡] Akimitsu Narita,[†] Xinliang Feng,^{||} and Klaus Müllen^{*,†}

[†]Max Planck Institute for Polymer Research, Ackermannweg 10, 55128, Mainz, Germany

[‡]Dipartimento di Chimica, Materiali ed Ingegneria Chimica ‘G. Natta’, Politecnico di Milano, Piazza Leonardo da Vinci 32, 20133 Milano, Italy

^{||}Center for Advancing Electronics Dresden (CFAED) & Department of Chemistry and Food Chemistry, Dresden University of Technology, Walther-Hempel-Bau Mommsenstrasse 4, 01062 Dresden, Germany

Supporting Information

ABSTRACT: We describe the first coronoid nanographene C216-molecule. As an extended polycyclic aromatic hydrocarbon containing a defined cavity, our molecule can be seen as a model system to study the influence of holes on the physical and chemical properties of graphene. Along the pathway of an eight-step synthesis including Yamamoto-type cyclization followed by 6-fold Diels–Alder cycloaddition, C216 was obtained by oxidative cyclodehydrogenation in the final step. The defined molecular structure with a cavity was unambiguously validated by MALDI-TOF mass spectrometry and FTIR, Raman, and UV–vis absorption spectroscopy coupled with DFT simulations.

Cycloarenes are macrocyclic conjugated compounds formed by circularly fused benzene rings, which enclose a cavity with inward-looking carbon–hydrogen bonds. The history of cycloarenes goes back to 1987, when the first example with 12 benzene rings, kekulene, was published by Staab and Diederich.¹ Numerous theoretical studies have targeted, for example, cycloarene aromaticity, vibrational frequencies, and magnetic susceptibility,² but kekulene and cyclo[*d,e,d,e,e,d,e,d,e,e*]decakisbenzene³ were the only two physical examples. Three decades later, in 2012, the third example of cycloarene, namely septulene with 14 benzene rings, was reported by King et al.⁴ Investigations of the electronic and structural properties of these cycloarenes suggest π -electron localized sextets rather than delocalized aromatic systems, thus supporting Clar’s model over the so-called kekulé structure.⁵ The known cycloarenes belong to the subgroup of primitive coronoids, having a hole surrounded by a single band of hexagons, as opposed to the, up until this publication, theoretical coronoids with more bands of hexagons.⁶ The geometry of coronoid molecules can be generally understood as polycyclic aromatic hydrocarbons (PAHs) with a cavity of at least two hexagons.^{6,7} Extended PAHs, such as C42 (with 42 sp^2 carbons; hexa-*peri*-hexabenzocoronene),⁸ C60,⁹ C96,¹⁰ and C222,¹¹ can be regarded as nanographene molecules, which hold promise for potential (opto-)electronic applications,¹² and also serve as defined model structures of graphene.¹³ Recently,

graphene with regular pores, which is called graphene nanomesh (GNM), has been demonstrated to have an open band gap, in contrast to zero-band gap graphene, highlighting the significant influence of the pore on the electronic features.¹⁴ The band gap of GNMs can be tuned by the diameter and density of the holes, showing p-type semiconducting properties.¹⁵ The formation of coronoids by introducing a defined cavity in nanographene molecules could thus be an efficient approach to modulate their optical and electronic properties without changing their external structures. Nevertheless, to the best of our knowledge, coronoid PAHs with more than one band of annelated rings have never been synthesized. Here, we report the first extended coronoid C216, containing 216 sp^2 carbons, which can be viewed as C222 with a “hole” of approximately 0.6 nm (Figure 1). The structure of C216 was unambiguously verified by a combination of matrix-assisted laser desorption/ionization time-of-flight (MALDI-TOF) mass spectrometry (MS) and FTIR, Raman, and UV–vis absorption

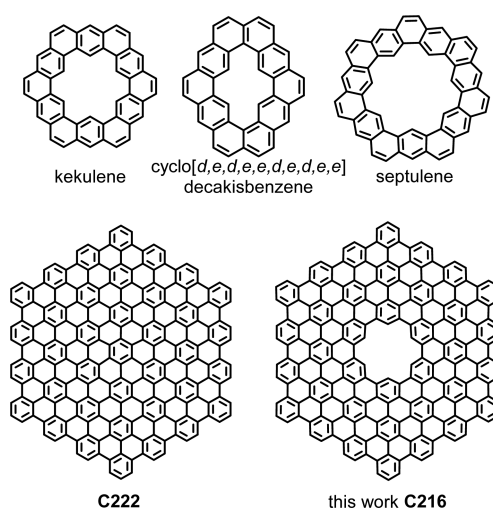


Figure 1. Structures of kekulene, cyclo[*d,e,d,e,e,d,e,d,e,e*]-decakisbenzene, septulene, C222, and coronoid C216.

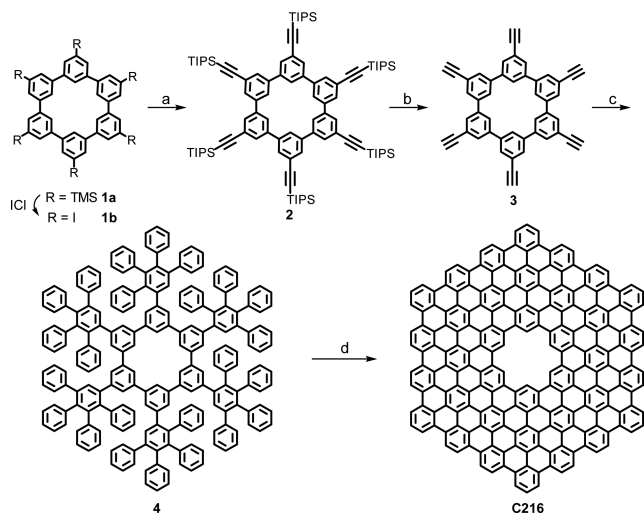
Received: February 1, 2016

Published: March 15, 2016

spectroscopic analyses, which were supported by theoretical studies. In particular, UV–vis absorption spectroscopy and density functional theory (DFT) calculations on **C216** and **C222** elucidated considerable effects of the cavity on their (opto-)electronic properties, including a sizable blue-shift of the absorption maximum of **C216** and an increase of the HOMO–LUMO gap, compared with that of **C222** (DFT: 0.4 eV).

The synthesis of coronoid **C216** was carried out as shown in **Scheme 1**. 5,5',5'',5''',5''''-Hexa-iodo-hexa-*m*-phenylene **1b**

Scheme 1. Synthetic Route Towards Coronoid **C216**^a



^aReagents and conditions: (a) CuI, PPh₃, Pd(PPh₃)₄, TIPS-acetylene, piperidine, 62%; (b) TBAF, THF, 78%; (c) 2,3,4,5-tetraphenylcyclopenta-2,4-dienone, *o*-xylene, 66%; (d) FeCl₃, DCM/CH₃NO₂, 84%.

was prepared as previously reported,¹⁶ through nickel(0)-mediated Yamamoto-type cyclization of 5,3''-dibromo-3,5',5''-tris-trimethylsilyl-[1,1';3',1'']terphenyl, giving the hexatrimethylsilyl-analogue **1a**, followed by a treatment with iodine monochloride. The extension of **1b** to polyphenylene dendrimer **4**, which serves as the precursor of **C216**, was started with 6-fold Hagihara–Sonogashira cross-coupling with tri(isopropyl)silyl (TIPS)-acetylene to afford hexakis-tri(isopropyl)silylethynyl-hexa-*m*-phenylene cycle **2**.¹⁷ Subsequently, deprotection of **2** with tetra-*n*-butylammonium fluoride (TBAF) yielded hardly soluble hexa-ethynyl-cyclohexa-*m*-phenylene **3**, which was subjected to microwave-assisted 6-fold Diels–Alder cycloaddition with 2,3,4,5-tetraphenylcyclopenta-2,4-dienone to afford precursor **4**. Polyphenylene **4** was purified via preparative recycling gel permeation chromatography and unambiguously characterized by ¹H and ¹³C NMR, H–H correlation spectroscopy, H–H nuclear overhauser enhancement spectroscopy, H–H total correlation spectroscopy, and high-resolution MALDI-TOF MS (**Figures 2a** and **S4–S9**). All the proton signals could be assigned with the help of 2D NMR spectroscopy verifying the structure of **4**. Finally, precursor **4** was “planarized” into **C216** through oxidative cyclodehydrogenation using iron(III) chloride. The cyclodehydrogenation of dendritic precursors has been extensively studied over the last two decades, which allowed for the synthesis of a number of PAHs, including **C222** as the largest example up to date.¹⁸ The cyclodehydrogenation of precursor **4** was initially attempted with 5 equiv of iron(III) chloride per hydrogen to be removed (5 equiv/H), but

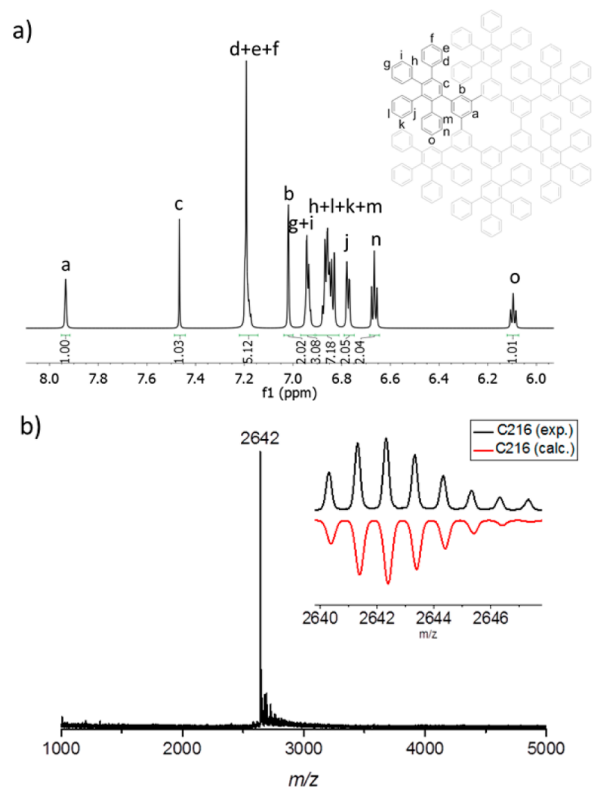


Figure 2. (a) ¹H NMR spectra of **4** and (b) MALDI-TOF spectrum of **C216**; inset: magnified spectrum showing isotopic distribution.

MALDI-TOF MS analysis indicated that the planarization was not complete, apparently stalling with 3 bonds missing, even after stirring for 3 days. The loading of iron(III) chloride was thus increased to 7.5 equiv/H, which led to the successful formation of **C216** after stirring for 3 days, as verified by MALDI-TOF MS analysis showing a peak at $m/z = 2640.3835$, consistent with the expected mass of **C216**, i.e., 2640.3756 (**Figure 2b**). However, partial chlorination could not be suppressed, similar to the previous synthesis of extended nanographenes.¹¹ The isotopic distribution observed for the obtained **C216** sample was in perfect agreement with the pattern simulated for C₂₁₆H₄₈, corroborating the complete cyclodehydrogenation (**Figure 2b**, inset). Coronoid **C216** was not soluble in organic solvents, which precluded characterization by NMR spectroscopy or growth of single crystals. Nevertheless, further structural proof could be obtained by micro-IR and micro-Raman spectroscopic analyses on powder samples of **C216**. **Figure 3a** shows the three characteristic IR bands associated with the C–H out-of-plane bending vibrations observed in **C216**. These are well accounted by DFT calculations which also reveal the associated nuclear displacements, localized on the three kinds of C–H bonds of **C216** (see **Supporting Information** (SI) for details). The band measured at 786 cm^{−1} is mostly due to the collective bending vibration of the CH bonds located at the six outer vertexes of **C216** and could be named as a TRIO mode, the band at 802 cm^{−1} is mostly due to the bending of the C–H bonds located along the six outer edges of **C216** (DUO mode).¹⁹ Most importantly, the band at 857 cm^{−1} is due to the collective bending of the C–H bonds at the inner edge of the hole in **C216** and thus constitutes a characteristic IR marker of this peculiar feature of the molecule. Although it is not conclusively mentioned in the literature, the “hole marker” peaks can also be

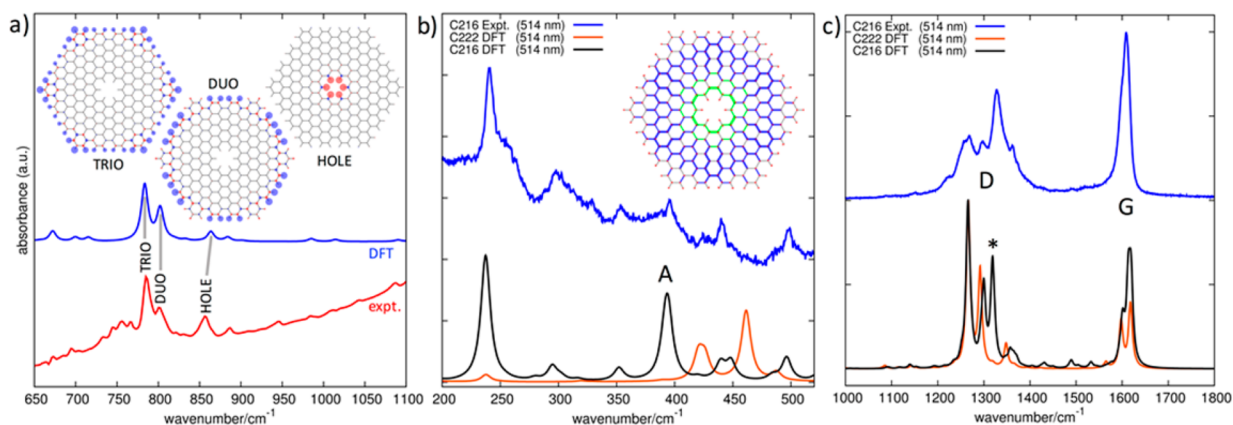


Figure 3. (a) IR spectrum of **C216** (red) compared with DFT calculation at the B3LYP/6-31G(d,p) (blue). (b,c) Micro-Raman spectrum of a powder sample of **C216** recorded with 514 nm excitation. The low-wavenumber region (b) and the first-order G and D peaks (c) are compared with results from DFT calculations at the B3LYP/6-31G(d,p). Calculations on the parent molecule **C222** are also reported for comparison (see text).

found in the FTIR spectra of kekulene and septulene.^{4,20} The Raman spectrum of **C216** in the solid state (Figure 3c) shows the main expected features of graphitic molecules, namely a structured D and G band.²¹ The comparison between DFT calculations for **C222** and **C216** highlights the presence of one mode in the D region (labeled with a star in Figure 3c) whose nuclear displacements are more localized at the hole edge. Such a prominent Raman line, which is also experimentally observed, is not seen in **C222** and can be taken as a signature of the hole. Further signature features are identified in the low-wavenumber region of the Raman spectrum, among which DFT calculations reveal the breathing mode of the hole (A-mode, Figure 3b). This is due to the contribution of two very close totally symmetric modes involving the collective contraction of the C–C bonds nearby the hole accompanied by the collective stretching of the outer C–C bonds.

Albeit the insoluble nature of coronoid **C216**, its UV–vis absorption spectrum could be measured from a chlorobenzene suspension by using an integration sphere (Figure 4). A closer look at the broad, nearly featureless absorption profile, by taking the second derivative, displayed subtle changes in the slope at 620, 520, and 450 nm, which might correspond to different optical transitions (bottom panel of Figure 4). TD-DFT calculations on **C216** at the B3LYP/6-31G(d,p) level indeed revealed doubly degenerate transitions at 613 and 519 nm as well as a cluster at 455, 439, 426, and 414 nm. This respectively corresponds to p -, β -, and β' -bands in Clar's notation and are consistent with the positions estimated from the experimental spectrum. In contrast, the absorption spectrum of **C222** features a broad absorption with maximum at ~ 750 nm.¹¹ TD-DFT calculation reveals that the p -band, which is generally the one most related to the HOMO–LUMO transition in PAHs, blue-shifts by about 100 nm (0.3 eV), when comparing **C222** (714 nm) with **C216** (613 nm).

Furthermore, DFT calculations on coronoid **C216** and **C222** gave more insight into the effect of the “hole”. The HOMO and LUMO levels of **C216** were revealed to be at -4.7 and -2.5 eV, respectively, with a HOMO–LUMO gap of 2.2 eV, while the HOMO and LUMO levels of **C222** are reported to be at -4.5 and -2.7 eV, respectively, with a HOMO–LUMO gap of 1.8 eV.²² This result demonstrated that the introduction of the hole in the **C222** disk increased the HOMO–LUMO gap by 0.4 eV (see Figure 5: decrease of the HOMO and increase of the LUMO by 0.2 eV), which is in agreement with the UV–vis

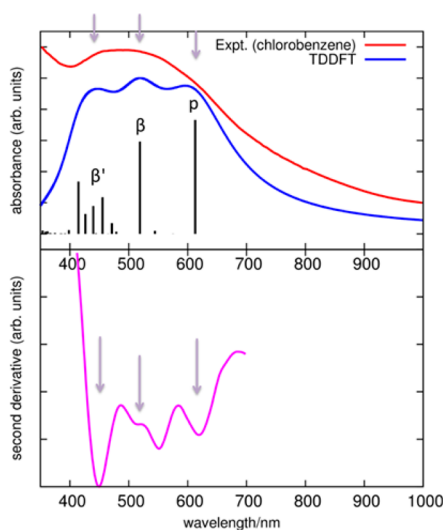


Figure 4. UV–vis absorption spectrum of **C216** in chlorobenzene suspension (top) with its second derivative (bottom). The arrows indicate the positions of the transitions determined by TD-DFT at the B3LYP/6-31G(d,p) level, which are also shown with black sticks whose length is proportional to the oscillator strength. The simulated absorption profile from TD-DFT transitions is also reported for comparison with experimental data.

measurement (see SI for the theoretical details, including the comparison of B3LYP, PBE0, and PBE functionals).

In summary, the synthesis and characterization of the first multilayer coronoid **C216** have been described. Investigations by MALDI-TOF MS and IR, Raman, and UV–vis absorption spectroscopy combined with (TD-)DFT calculations provided an explicit structure proof. The FTIR and Raman spectra were starkly modulated by the introduction of the cavity, compared to those of the parent **C222** disk. Notably FTIR analysis of coronoid **C216** revealed a fingerprint peak from C–H bonds inside the cavity, which can serve as a “hole marker”. Furthermore, the formation of coronoids offers a new approach to fine-tune the (opto-)electronic properties of nanographene molecules, as demonstrated by the increase of the HOMO–LUMO gap from **C222** to **C216**. Such coronoids can also serve as model structures of GNMs, which would help elucidate the exact effect of the cavity on the graphene structure.

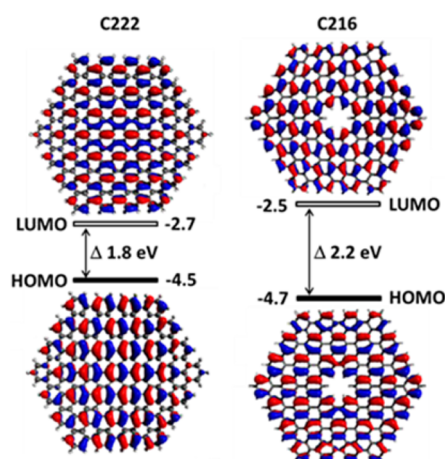


Figure 5. HOMO and LUMO levels and HOMO–LUMO gap for C222 and C216 calculated by DFT at the B3LYP/6-31G(d,p) level (see SI for details).

■ ASSOCIATED CONTENT

Supporting Information

The Supporting Information is available free of charge on the ACS Publications website at DOI: 10.1021/jacs.6b01181.

Experimental details and data (PDF)

■ AUTHOR INFORMATION

Corresponding Author

*muellen@mpip-mainz.mpg.de

Present Address

§BASF SE, 67056 Ludwigshafen, Germany

Notes

The authors declare no competing financial interest.

■ ACKNOWLEDGMENTS

We are grateful for the financial support from the European Research Council grant on NANOGRAPH, DFG Priority Program SPP 1459, European Commission through the FET-Proactive Project “MoQuaS”, contract no. 610449, and Graphene Flagship (no. CNECT-ICT-604391). We thank Wen Zhang for high-resolution MALDI-TOF MS analysis and Prof. Mark D. Watson for insightful comments on the manuscript.

■ REFERENCES

- (1) Staab, H. A.; Diederich, F. *Chem. Ber.* **1983**, *116*, 3487.
- (2) (a) Dias, J. R. *J. Phys. Chem. A* **2008**, *112*, 12281. (b) Miyoshi, H.; Nobusue, S.; Shimizu, A.; Tobe, Y. *Chem. Soc. Rev.* **2015**, *44*, 6560.
- (3) Funhoff, D. J. H.; Staab, H. A. *Angew. Chem., Int. Ed. Engl.* **1986**, *25*, 742.
- (4) Kumar, B.; Viboh, R. L.; Bonifacio, M. C.; Thompson, W. B.; Buttrick, J. C.; Westlake, B. C.; Kim, M.-S.; Zoellner, R. W.; Varganov, S. A.; Mörschel, P.; Teteruk, J.; Schmidt, M. U.; King, B. T. *Angew. Chem., Int. Ed.* **2012**, *51*, 12795.
- (5) (a) Aihara, J.-i.; Makino, M.; Ishida, T.; Dias, J. R. *J. Phys. Chem. A* **2013**, *117*, 4688. (b) Hajgató, B.; Deleuze, M. S.; Ohno, K. *Chem. - Eur. J.* **2006**, *12*, 5757.
- (6) Cyvin, S. J.; Brunvoll, J.; Cyvin, B. N. *J. Chem. Inf. Model.* **1990**, *30*, 210.
- (7) (a) Cyvin, S. J.; Brunvoll, J.; Cyvin, B. N. *In Theory of Coronoid Hydrocarbons*; Springer: Berlin, 1991; Vol. 54, p 13. (b) Brunvoll, J.; Cyvin, B. N.; Cyvin, S. J.; Gutman, I.; Tošić, R.; Kovačević, M. *J. Mol. Struct.: THEOCHEM* **1989**, *184*, 165.

(8) Kubel, C.; Eckhardt, K.; Enkelmann, V.; Wegner, G.; Müllen, K. *J. Mater. Chem.* **2000**, *10*, 879.

(9) Feng, X.; Liu, M.; Pisula, W.; Takase, M.; Li, J.; Müllen, K. *Adv. Mater.* **2008**, *20*, 2684.

(10) Tomović, Ž.; Watson, M. D.; Müllen, K. *Angew. Chem., Int. Ed.* **2004**, *43*, 755.

(11) Simpson, C. D.; Brand, J. D.; Berresheim, A. J.; Przybilla, L.; Räder, H. J.; Müllen, K. *Chem. - Eur. J.* **2002**, *8*, 1424.

(12) (a) Laschat, S.; Baro, A.; Steinke, N.; Giesselmann, F.; Hägele, C.; Scalia, G.; Judele, R.; Kapatsina, E.; Sauer, S.; Schreivogel, A.; Tosoni, M. *Angew. Chem., Int. Ed.* **2007**, *46*, 4832. (b) Schmidtke, J. P.; Friend, R. H.; Kastler, M.; Müllen, K. *J. Chem. Phys.* **2006**, *124*, 174704. (c) Debad, J. D.; Morris, J. C.; Magnus, P.; Bard, A. J. *J. Org. Chem.* **1997**, *62*, 530. (d) Pisula, W.; Menon, A.; Stepputat, M.; Lieberwirth, I.; Kolb, U.; Tracz, A.; Sirringhaus, H.; Pakula, T.; Müllen, K. *Adv. Mater.* **2005**, *17*, 684.

(13) (a) Morita, Y.; Suzuki, S.; Sato, K.; Takui, T. *Nat. Chem.* **2011**, *3*, 197. (b) Pisula, W.; Feng, X.; Müllen, K. *Chem. Mater.* **2011**, *23*, 554. (c) Banerjee, S.; Bhattacharyya, D. *Comput. Mater. Sci.* **2008**, *44*, 41. (d) Ball, M.; Zhong, Y.; Wu, Y.; Schenck, C.; Ng, F.; Steigerwald, M.; Xiao, S.; Nuckolls, C. *Acc. Chem. Res.* **2015**, *48*, 267. (e) Kastler, M.; Schmidt, J.; Pisula, W.; Sebastiani, D.; Müllen, K. *J. Am. Chem. Soc.* **2006**, *128*, 9526.

(14) (a) Zeng, Z.; Huang, X.; Yin, Z.; Li, H.; Chen, Y.; Li, H.; Zhang, Q.; Ma, J.; Boey, F.; Zhang, H. *Adv. Mater.* **2012**, *24*, 4138. (b) Liang, X.; Jung, Y.-S.; Wu, S.; Ismach, A.; Olynick, D. L.; Cabrini, S.; Bokor, J. *Nano Lett.* **2010**, *10*, 2454. (c) Bai, J.; Zhong, X.; Jiang, S.; Huang, Y.; Duan, X. *Nat. Nanotechnol.* **2010**, *5*, 190. (d) Yang, J.; Ma, M.; Li, L.; Zhang, Y.; Huang, W.; Dong, X. *Nanoscale* **2014**, *6*, 13301. (e) Zhao, Y.; Hu, C.; Song, L.; Wang, L.; Shi, G.; Dai, L.; Qu, L. *Energy Environ. Sci.* **2014**, *7*, 1913. (f) Ning, G.; Fan, Z.; Wang, G.; Gao, J.; Qian, W.; Wei, F. *Chem. Commun.* **2011**, *47*, 5976. (h) Stile, P.; Szendrő, M.; Magda, G. Z.; Hwang, C.; Tapasztó, L. *Nano Lett.* **2015**, *15* (12), 8295–8299. (j) Robertson, A. W.; Lee, G.-D.; He, K.; Gong, C.; Chen, Q.; Yoon, E.; Kirkland, A. I.; Warner, J. H. *ACS Nano* **2015**, *9* (12), 11599–11607.

(15) (a) Jariwala, D.; Srivastava, A.; Ajayan, P. M. *J. Nanosci. Nanotechnol.* **2011**, *11*, 6621. (b) Wang, M.; Fu, L.; Gan, L.; Zhang, C.; Rummeli, M.; Bachmatiuk, A.; Huang, K.; Fang, Y.; Liu, Z. *Sci. Rep.* **2013**, *3*, 1238.

(16) Pisula, W.; Kastler, M.; Yang, C.; Enkelmann, V.; Müllen, K. *Chem. - Asian J.* **2007**, *2*, 51.

(17) Wu, J.; Watson, M. D.; Zhang, L.; Wang, Z.; Müllen, K. *J. Am. Chem. Soc.* **2004**, *126*, 177.

(18) (a) Wu, J.; Tomović, Ž.; Enkelmann, V.; Müllen, K. *J. Org. Chem.* **2004**, *69*, 5179. (b) Iyer, V. S.; Wehmeier, M.; Brand, J. D.; Keegstra, M. A.; Müllen, K. *Angew. Chem., Int. Ed. Engl.* **1997**, *36*, 1604. Wu, J.; Pisula, W.; Müllen, K. *Chem. Rev.* **2007**, *107*, 718. Narita, A.; Wang, X.-Y.; Feng, X.; Müllen, K. *Chem. Soc. Rev.* **2015**, *44*, 6616.

(19) Tommasini, M.; Lucotti, A.; Alfè, M.; Ciajolo, A.; Zerbi, G. *Spectrochim. Acta, Part A* **2016**, *152*, 134.

(20) Balm, S. P.; Kroto, H. W.; Mon, R. *Mon. Not. R. Astron. Soc.* **1990**, *245*, 193.

(21) Maghsoumi, A.; Brambilla, L.; Castiglioni, C.; Müllen, K.; Tommasini, M. *J. Raman Spectrosc.* **2015**, *46*, 757.

(22) Moran, D.; Stahl, F.; Bettinger, H. F.; Schaefer, H. F.; Schleyer, P. v. R. *J. Am. Chem. Soc.* **2003**, *125*, 6746.